

目次

持久性、迁移性和潜在毒性化学品环境健康风险与控制研究现状及趋势分析 张少轩, 陈安娜, 陈成康, 景侨楠, 刘建国 (3017)

我国厨余垃圾资源化技术的多维绩效评价 杨光, 史波芬, 周传斌 (3024)

基于 MSPA 和电路理论的京津冀城市群热环境空间网络 乔治, 陈嘉悦, 王楠, 卢应爽, 贺瞳, 孙宗耀, 徐新良, 杨浩, 李莹, 王方 (3034)

城市空间格局与热环境响应关系:以合肥市为例 陈媛媛, 姚侠妹, 偶春, 张清怡, 姚晓洁 (3043)

天津市“十三五”期间 PM_{2.5} 减排效果评估 肖致美, 徐虹, 蔡子颖, 张裕芬, 刘茂辉, 孙猛, 李鹏, 杨宁, 戴运峰 (3054)

清洁取暖对保定市采暖期 PM_{2.5} 中碳质气溶胶的影响 罗宇睿, 张凯, 赵好希, 任家豪, 段菁春, 李欢欢, 关健, 郭志强, 李博文 (3063)

南京地区细颗粒物污染输送影响及潜在源区 谢放尖, 郑新梅, 窦焱焱, 杨峰, 刘春蕾, 李洁, 谢轶嵩, 王艳, 胡建林, 陈长虹 (3071)

大气环流型对珠三角 2015~2020 年臭氧变化的影响 汪瑶, 刘润, 辛繁 (3080)

热带气旋对海南岛臭氧污染的影响分析 符传博, 丹利, 佟金鹤, 徐文帅 (3089)

基于 CMAQ 和 HYSPLIT 模式的日照市夏季臭氧污染成因和来源分析 林鑫, 全纪龙, 王伊凡, 陈羽翔, 刘永乐, 张鑫, 敖丛杰, 刘浩天 (3098)

2016~2020 年成都市控制 PM_{2.5} 和 O₃ 污染的健康效益评价 张莹, 田琪琪, 魏晓钰, 张少波, 胡文东, 李明刚 (3108)

深圳市 2022 年春季新冠疫情管控期间空气质量分析 刘婵芳, 张傲星, 房庆, 叶毓婧, 杨红龙, 陈炯恺, 吴雯潞, 侯岳, 莫佳佳, 傅宗攻 (3117)

贵州省生物质燃烧源大气污染物排放清单 王艳妮, 杨敬婷, 黄贤峰, 程燕, 陆标, 顾兆林 (3130)

西安市大气降水的主要化学组分及其来源 周东, 黄智浦, 李思敏, 王森, 牛振川, 熊晓虎, 冯雪 (3142)

宜昌市大气微塑料的分布、呼吸暴露及溯源 刘立明, 王超, 巩文雯, 陆安祥, 任东, 涂清, 贾漫珂 (3152)

雅鲁藏布江水化学演变规律 江平, 张全发, 李思悦 (3165)

无定河流域地表水硝酸盐浓度的时空分布特征及来源解析 徐奇峰, 夏云, 李书鉴, 王万洲, 李志 (3174)

太浦河水体与沉积物中重金属的季节变化特征与污染评价 罗鹏程, 涂耀仁, 孙婷婷, 刘生辉, 高佳欣, 寇佳怡, 顾心彤, 段艳平 (3184)

北京市北运河水体中抗生素污染特征及风险评估 蒋宝, 隋珊珊, 孙成一, 王亚玲, 荆降龙, 凌文翠, 李珊珊, 李国傲 (3198)

氮和氧同位素示踪伊洛河河水硝酸盐来源及转化过程 郭文静, 张东, 蒋浩, 吴洋洋, 张郭妙, 段慧真, 许梦军, 麻冰涓, 陈昊, 黄兴宇 (3206)

淮河下游湖泊表层水和沉积物中 PPCPs 分布特征及风险评估 武宇圣, 黄天寅, 张家根, 田永静, 庞燕, 许秋瑾 (3217)

西宁市浅层地下水化学特征及形成机制 刘春燕, 于开宁, 张英, 荆继红, 刘景涛 (3228)

叶尔羌河流域平原区地下水污染风险评价 闫志云, 曾妍妍, 周金龙, 孙英, 马常莲 (3237)

密云水库细菌群落组成结构及影响因素 陈颖, 王佳文, 梁恩航, 陈倩 (3247)

可见光激发下模拟海水中四环素光降解的机制和路径 许恒韬, 付小航, 丰卫华, 王挺 (3260)

纳米零价铁改性生物炭对水中氨氮的吸附特性及机制 陈文静, 石峻岭, 李雪婷, 张李金, 刘富强, 陈正祝, 庞维海, 杨殿海 (3270)

高锰酸钾改性椰壳生物炭对水中 Cd(II) 和 Ni(II) 的去除性能及机制 张凤智, 王敦球, 曹星洋, 刘桥京, 岳甜甜, 刘立恒 (3278)

铜改性净水污泥水热炭对水体中磷的吸附特性及底泥内源磷的固定 何李文泽, 陈钰, 孙飞, 李艳君, 杨顺生, 张志鹏 (3288)

城镇生活污水处理厂出水硝酸盐浓度及同位素组成的影响因素 张东, 葛文彪, 赵爱萍, 高振朋, 陈昊, 张琮, 蒋浩, 吴文阳, 廖琪, 李成杰, 黄兴宇, 麻冰涓 (3301)

基于 Meta 分析的污水处理工艺对微塑料去除效果影响 符立松, 侯磊, 王艳霞, 李晓琳, 王万宾, 梁启斌 (3309)

我国自然生态系统氮沉降临界负荷评估 黄静文, 刘磊, 顾晓元, 凌超普 (3321)

气候变化和人类活动对东部沿海地区 NDVI 变化的影响分析 金岩松, 金凯, 王飞, 刘春霞, 秦鹏, 宗全利, 刘佩茹, 陈明利 (3329)

基于 InVEST 模型和 PLUS 模型的环杭州湾生态系统碳储量 丁岳, 王柳柱, 桂峰, 赵晨, 朱望远 (3343)

河西走廊中段荒漠绿洲土壤生态学计量特征 孙雪, 龙永丽, 刘乐, 刘继亮, 金丽琼, 杜海峰, 陈凌云 (3353)

乌梁素海东部流域非生长季草地土壤细菌群落结构的垂向差异 李文宝, 张博尧, 史玉娇, 郭鑫, 李兴月 (3364)

芦芽山华北落叶松林土壤剖面细菌群落分布格局 毛晓雅, 刘晋仙, 贾彤, 吴铁航, 柴宝峰 (3376)

植被类型对黄土高原露天复垦土壤碳循环功能基因的影响 赵蛟, 马静, 朱燕峰, 于昊辰, 张琦, 陈浮 (3386)

施用生物炭对麦田土壤细菌群落多样性和冬小麦生长的影响 姚丽茹, 李伟, 朱良正, 曹布仓, 韩娟 (3396)

甜龙竹不同种植年限对土壤真菌群落的影响 朱书红, 辉朝茂, 赵秀婷, 刘蔚漪, 张仲富, 刘会会, 张文君, 朱礼月, 涂丹丹 (3408)

生物炭对热带地区辣椒种植土壤 N₂O 排放及其功能基因的影响 陈琦琦, 王紫君, 陈云忠, 王誉琴, 朱启林, 胡天怡, 胡煜杰, 伍延正, 孟磊, 汤水荣 (3418)

覆膜和有机无机配施对夏玉米农田温室气体排放及水氮利用的影响 蒋洪雨, 雷琪, 张彪, 吴淑芳 (3426)

不同类型地膜覆盖对土壤质量、根系生长和产量的影响 穆晓国, 高虎, 李梅花, 赵欣茹, 郭宁, 靳磊, 李建设, 叶林 (3439)

基于 PMF 模型的某铅锌冶炼城市降尘重金属污染评价及来源解析 陈明, 王琳玲, 曹柳, 李名闯, 申哲民 (3450)

云南 5 城市道路扬尘 PM_{2.5} 中重金属含量表征及健康风险 韩新宇, 郭晋源, 史建武, 李定霜, 王怡明, 宁平 (3463)

兰州市黄河风情线地表积尘及周边绿地土壤重金属污染特征及风险评价 李军, 李开明, 王晓槐, 焦亮, 臧飞, 毛潇萱, 杨云钦, 台喜生 (3475)

PMF 和 RF 模型联用的土壤重金属污染来源解析与污染评价:以西北某典型工业园区为例 高越, 吕童, 张鑫凯, 张博哈, 毕思琪, 周旭, 张炜, 曹红斌, 韩增玉 (3488)

基于 APCS-MLR 受体模型和地统计法的矿区周边农用地土壤重金属来源解析 张传华, 王钟书, 刘力, 刘燕 (3500)

PCA-APCS-MLR 和地统计学的典型农田土壤重金属来源解析 王美华 (3509)

三峡库区稻田土壤重金属污染特征及风险评价 刘娅君, 李彩霞, 梅楠, 张美平, 张成, 王定勇 (3520)

皖江经济带耕地重金属健康风险评价及环境基准 刘海, 魏伟, 潘海, 宋阳, 靳磊, 李建设, 叶林 (3531)

张家口市万全区某种植区土壤重金属污染评价与来源分析 安永龙, 殷秀兰, 李文娟, 金爱芳, 鲁青原 (3544)

滁州市表层土壤重金属含量特征、源解析及污染评价 汤金来, 赵宽, 胡睿鑫, 徐涛, 王宜萱, 杨扬, 周葆华 (3562)

矿业废弃地重金属形态分布特征与迁移转化影响机制分析 魏洪斌, 罗明, 向奎, 查理思, 杨慧丽 (3573)

基于成土母质的矿产资源基地土壤重金属生态风险评价与来源解析 卫晓峰, 孙紫坚, 陈自然, 魏浩, 孙厚云, 刘卫, 傅大庆 (3585)

不同种类蔬菜重金属富集特征及健康风险 祁浩, 庄坚, 庄重, 王琪, 万亚男, 李花粉 (3600)

山东省典型灌溉区土壤-小麦重金属健康风险评估 王菲, 费敏, 韩冬锐, 李春芳, 曹文涛, 姚磊, 曹见飞, 吴泉源 (3609)

基于机器学习方法的小麦镉富集因子预测 牛硕, 李艳玲, 杨阳, 商艳萍, 王天齐, 陈卫平 (3619)

《环境科学》征订启事(3062) 《环境科学》征稿简则(3116) 信息(3164, 3259, 3572)

高锰酸钾改性椰壳生物炭对水中Cd(II)和Ni(II)的去除性能及机制

张凤智¹, 王敦球^{1,2,3}, 曹星泮¹, 刘桥京¹, 岳甜甜¹, 刘立恒^{1,2,3*}

(1. 桂林理工大学环境科学与工程学院, 桂林 541006; 2. 桂林理工大学岩溶地区水污染控制与用水安全保障协同创新中心, 桂林 541006; 3. 桂林理工大学广西环境污染控制理论与技术重点实验室, 桂林 541006)

摘要: 以高锰酸钾改性商业椰壳生物炭(MCBC)为吸附剂,探讨了它对Cd(II)和Ni(II)的去除性能及机制。当初始pH和MCBC投加量分别为5和3.0 g·L⁻¹时,Cd(II)和Ni(II)的去除率均高于99%。Cd(II)和Ni(II)的去除更符合准二级动力学模型,表明它们的去除以化学吸附为主;Cd(II)和Ni(II)去除的控速步骤为快速去除阶段,而该阶段的速率取决于液膜扩散和颗粒内扩散(表面扩散)。Cd(II)和Ni(II)主要通过表面吸附和孔隙填充附着在MCBC上,表面吸附的贡献更大;MCBC对Cd(II)和Ni(II)的饱和吸附量分别为57.18 mg·g⁻¹和23.29 mg·g⁻¹,约为前驱体(椰壳生物炭)的5.74倍和6.97倍。Cd(II)和Ni(II)的去除是自发的、吸热的,具有较为明显的化学吸附热力学特征。Cd(II)通过离子交换、共沉淀、络合反应和阳离子- π 相互作用附着在MCBC上;而Ni(II)则是通过离子交换、共沉淀、络合反应和氧化还原反应被MCBC去除;其中,共沉淀和络合作用是Cd(II)和Ni(II)表面吸附的主要方式,且络合产物中无定形的Mn—O—Cd或Mn—O—Ni的占比可能会较高。研究结果将为商业生物炭在重金属废水处理中的实际应用提供重要的技术支持和理论依据。

关键词: 高锰酸钾改性; 椰壳生物炭(MCBC); Cd(II)和Ni(II); 吸附; 去除性能及机制

中图分类号: X703.1 文献标识码: A 文章编号: 0250-3301(2023)06-3278-10 DOI: 10.13227/j.hjkk.202207235

Removal Performance and Mechanism of Potassium Permanganate Modified Coconut Shell Biochar for Cd(II) and Ni(II) in Aquatic Environment

ZHANG Feng-zhi¹, WANG Dun-qiu^{1,2,3}, CAO Xing-feng¹, LIU Qiao-jing¹, YUE Tian-tian¹, LIU Li-heng^{1,2,3*}

(1. College of Environmental Science and Engineering, Guilin University of Technology, Guilin 541006, China; 2. Collaborative Innovation Center for Water Pollution Control and Water Safety in Karst Area, Guilin University of Technology, Guilin 541006, China; 3. Guangxi Key Laboratory of Environmental Pollution Control Theory and Technology, Guilin University of Technology, Guilin 541006, China)

Abstract: In this study, coconut shell biochar modified by KMnO₄ (MCBC) was used as the adsorbent, and its removal performance and mechanism for Cd(II) and Ni(II) were discussed. When the initial pH and MCBC dosage were separately 5 and 3.0 g·L⁻¹, respectively, the removal efficiencies of Cd(II) and Ni(II) were both higher than 99%. The removal of Cd(II) and Ni(II) was more in line with the pseudo-second-order kinetic model, indicating that their removal was dominated by chemisorption. The rate-controlling step for Cd(II) and Ni(II) removal was the fast removal stage, for which the rate depended on the liquid film diffusion and intraparticle diffusion (surface diffusion). Cd(II) and Ni(II) were mainly attached to the MCBC via surface adsorption and pore filling, in which the contribution of surface adsorption was greater. The maximum adsorption amounts of Cd(II) and Ni(II) by MCBC were individually 57.18 mg·g⁻¹ and 23.29 mg·g⁻¹, which were approximately 5.74 and 6.97 times that of the precursor (coconut shell biochar), respectively. The removal of Cd(II) and Ni(II) was spontaneous and endothermic and had obvious thermodynamic characteristics of chemisorption. Cd(II) was attached to MCBC through ion exchange, co-precipitation, complexation reaction, and cation- π interaction, whereas Ni(II) was removed by MCBC via ion exchange, co-precipitation, complexation reaction, and redox. Among them, co-precipitation and complexation were the main modes of surface adsorption of Cd(II) and Ni(II). Additionally, the proportion of amorphous Mn—O—Cd or Mn—O—Ni in the complex may have been higher. These research results will provide important technical support and theoretical basis for the practical application of commercial biochar in the treatment of heavy metal wastewater.

Key words: potassium permanganate modification; coconut shell biochar(MCBC); Cd(II) and Ni(II); adsorption; removal performance and mechanism

随着金属矿开采、冶炼加工和机械制造等行业的快速发展,大量含镉和镍废水被排入水环境中,镉和镍的污染已成为一个严重的环境问题^[1-4]。在自然环境中,镉和镍具有不可降解性,并能在生物体内积累,导致其对生态系统的威胁更为严重。因此,对含镉和镍的废水进行有效处理是非常必要的。目前,含镉和镍废水的处理方法主要有化学沉淀法、电化学法、吸附法、离子交换法和膜分离法等^[5-8]。其中,吸附法由于操作简单、成本低和处理效率高等优点,被列为最有前途的重金属废水处理技术^[9]。

对于吸附法,污染物的成功去除取决于对目标污染物具有显著亲和力及快速吸附速率的吸附剂的选择^[10]。有研究证明,碳基材料(如碳纳米管、石墨烯、生物炭)非常适合作为重金属废水处理的吸附

收稿日期: 2022-07-24; 修订日期: 2022-08-16

基金项目: 国家自然科学基金项目(51638006,52160016); 广西高等学校高水平创新团队及卓越学者计划项目(002401013001); 广西重点实验室研究基金项目(桂科能1401Z004,桂科能1801Z009); 广西“八桂学者”岗位专项经费项目(2016A10)

作者简介: 张凤智(1996~),男,硕士研究生,主要研究方向为重金属废水处理, E-mail: 879400706@qq.com

* 通信作者, E-mail: deanhenry_liu01@126.com

剂^[11,12]. 其中,生物炭具有非常明显的成本优势,使其在重金属废水处理实际应用中有更大的潜力. 然而,生物炭对重金属离子的去除也存在吸附容量相对较低,吸附选择性较差等不足^[13]. 本课题组前期研究显示,椰壳生物炭对Cd(II)和Ni(II)的吸附容量分别仅为 $9.96 \text{ mg}\cdot\text{g}^{-1}$ 和 $3.34 \text{ mg}\cdot\text{g}^{-1}$. 因此,提高生物炭对重金属的吸附性能是实现其实际应用的重要前提.

有报道指出,改性是提高生物炭对重金属吸附性能的最为有效的途径之一^[14]. 生物炭的改性方法大体可分为化学改性、物理改性、负载矿物和磁性改性这 4 类^[15]. 与其他的改性方法相比, KMnO_4 化学改性不但能够显著地改善生物炭的孔隙性质,增加含氧官能团的数量,还能将锰氧化物负载到生物炭上,从而加强生物炭与重金属离子之间的相互作用,更显著地提高生物炭对重金属的吸附性能^[16].

本研究以高锰酸钾改性的椰壳生物炭为吸附剂,考察了溶液 pH 和吸附剂投加量对其吸附 Cd(II)和Ni(II)性能的影响;通过动力学、等温线和热力学分析,并结合生物炭的表征,探讨了 Cd(II)和Ni(II)去除的机制,以期为商业生物炭在重金属废水处理中的实际应用提供技术支持和理论依据.

1 材料与实验

1.1 实验材料

本实验使用的主要化学药剂 [$\text{Cd}(\text{NO}_3)_2 \cdot 4\text{H}_2\text{O}$ 、 $\text{Ni}(\text{NO}_3)_2 \cdot 6\text{H}_2\text{O}$ 、 KMnO_4 、 NaOH 和 HCl] 购自西陇科学股份有限公司,其纯度均为分析纯.

1.2 KMnO_4 改性椰壳生物炭的制备

KMnO_4 改性椰壳生物炭(MCBC)的制备流程如下:①将市售椰壳生物炭(20~30目)用去离子水反复洗涤5次,并在 105°C 的烘箱中干燥 12 h 后备用;②将干燥后的椰壳生物炭与 $0.9 \text{ mol}\cdot\text{L}^{-1}$ 的 KMnO_4 溶液充分混合(固液比为 1:20)后,在 90°C 下搅拌 2 h;③将生物炭用去离子水反复洗涤 5 次后,并在 70°C 下干燥 12 h. MCBC 的比表面积为 $509.8 \text{ m}^2\cdot\text{g}^{-1}$.

1.3 吸附实验

首先,称取一定质量的 MCBC ($0.01 \sim 0.3 \text{ g}$),置于装有 50 mL Cd(II)或Ni(II)溶液(初始浓度: $10 \sim 200 \text{ mg}\cdot\text{L}^{-1}$; 初始 pH: $2 \sim 8$)的聚丙烯离心管中. 然后,将离心管放入气浴恒温振荡器(ZD-85, 中国金逸; 转速为 $220 \text{ r}\cdot\text{min}^{-1}$)中,在不同温度下 (298 、 308 和 318 K) 振荡一定时间 ($0 \sim 24 \text{ h}$). 最

后,采用电感耦合等离子体发射光谱仪(7000DV, 美国 PE 公司)测定离心处理后上清液中 Cd(II)或 Ni(II)的浓度,并通过式(1)和式(2)分别计算它们的吸附量(q_t , $\text{mg}\cdot\text{L}^{-1}$)和去除率(φ , %).

$$q_t = 0.05 \times (c_0 - c_t) / m \quad (1)$$

$$\varphi = (c_0 - c_t) / c_0 \times 100\% \quad (2)$$

式中, c_0 为 Cd(II)或Ni(II)的初始浓度, $\text{mg}\cdot\text{L}^{-1}$; c_t 为 t 时刻 Cd(II)或Ni(II)的浓度, $\text{mg}\cdot\text{L}^{-1}$; m 为 MCBC 的质量, g .

1.4 动力学、等温线和热力学模型

1.4.1 动力学模型

采用准一级动力学模型(PFO)、准二级动力学模型(PSO)、液膜扩散模型(LFD)和颗粒内扩散模型(IpD)来分析 MCBC 去除 Cd(II)和Ni(II)的动力学. 上述动力学模型的公式如下^[17]:

$$q_t = q_e \cdot [1 - \exp(-k_1 \cdot t)] \quad (3)$$

$$q_t = q_e^2 \cdot k_2 \cdot t / (1 + q_e \cdot k_2 \cdot t) \quad (4)$$

$$\ln(1 - q_t/q_e) = -k_{\text{LFD}} \cdot t + A_L \quad (5)$$

$$q_t = k_{\text{IpD}} \cdot t^{0.5} + A_1 \quad (6)$$

式中, t 为吸附时间 h ; k_1 、 k_2 、 k_{LFD} 和 k_{IpD} 分别为准一级动力学模型、准二级动力学模型、液膜扩散模型和颗粒内扩散模型的速率常数,单位分别为 h^{-1} 、 $\text{g}\cdot(\text{mg}\cdot\text{h})^{-1}$ 、 h^{-1} 和 $\text{g}\cdot(\text{mg}\cdot\text{h}^{0.5})^{-1}$; A_L 为液膜扩散模型常数; A_1 为边界层特征常数.

1.4.2 等温线模型

采用 Langmuir、Freundlich 和 Temkin 模型对 MCBC 吸附 Cd(II)和Ni(II)的等温过程进行拟合分析,其数学表达式分别为^[18]:

$$q_e = q_{\text{max}} \cdot K_L \cdot c_e / (1 + K_L \cdot c_e) \quad (7)$$

$$q_e = K_F \cdot c_e^{1/n} \quad (8)$$

$$q_e = (R \cdot T / b_T) \cdot \ln(k_T \cdot c_e) \quad (9)$$

式中, q_e 为吸附剂对吸附质平衡时的吸附量, $\text{mg}\cdot\text{g}^{-1}$; q_{max} 为饱和吸附量, $\text{mg}\cdot\text{g}^{-1}$; K_L 为 Langmuir 模型的吸附常数, $\text{L}\cdot\text{g}^{-1}$; K_F 为 Freundlich 模型的吸附容量, $(\text{mg}\cdot\text{g}^{-1}) \cdot (\text{mg}\cdot\text{L}^{-1})^{-1/n}$; n 为 Freundlich 模型吸附常数; R 为理想气体常数, $8.314 \text{ J}\cdot(\text{mol}\cdot\text{K})^{-1}$; T 为热力学温度, K ; k_T 为平衡结合常数, $\text{L}\cdot\text{mg}^{-1}$; b_T 为与吸附热有关的 Temkin 常数, $\text{J}\cdot\text{mol}^{-1}$.

1.4.3 热力学

通过吉布斯自由能变 (ΔG^θ , $\text{kJ}\cdot\text{mol}^{-1}$)、焓变 (ΔH^θ , $\text{kJ}\cdot\text{mol}^{-1}$) 和熵变 [ΔS^θ , $\text{J}\cdot(\text{mol}\cdot\text{K})^{-1}$] 来研究 MCBC 去除 Cd(II)和Ni(II)的热力学特性. ΔG^θ 、 ΔH^θ 和 ΔS^θ 可通过以下方程确定^[19].

$$\Delta G^\theta = -R \cdot T \cdot \ln(1000 \cdot K_D) \quad (10)$$

$$\Delta G^\theta = \Delta H^\theta - T \cdot \Delta S^\theta \quad (11)$$

式中, K_D 为平衡因子(q_e/c_e)。

1.5 生物炭的表征

采用 X 射线衍射仪(XRD; X'Pert PRO, 荷兰帕纳科公司)、扫描电子显微镜及(SEM)、X 射线能量色散光谱仪(EDS, Zeiss meilin compact)、傅里叶变换红外光谱仪(FTIR; Nicolet. iS10, 美国赛默飞世尔科技)和 X 射线光电子能谱仪(XPS; thermo scientific ESCALAB 250 Xi)对Cd(II)和Ni(II)去除前后的 MCBC 的晶形结构、表面形貌及元素分布、表面官能团和元素形态进行表征。

2 结果与讨论

2.1 Cd(II)和Ni(II)的去除性能

2.1.1 初始 pH 的影响

不同初始 pH 下, MCBC 对Cd(II)和Ni(II)的去除性能如图 1(a)和图 1(b)所示. 在本研究范围内, 随着初始 pH 的升高, MCBC 对Cd(II)和Ni(II)的吸附量和去除效率均总体呈上升趋势; 而当初始 pH 大于 4 或 5 后, 这种增长趋势变得十分缓慢. 一般而言, 初始 pH 值决定了吸附剂表面电荷和溶液中污染物的形态分布, 进而影响污染物的去除性能^[18]. 根据Cd(II)和Ni(II)形态分布可知^[20], 在本研究的初始 pH 范围内, Cd(II)和Ni(II)的形态基本没有改变, 也就意味着 MCBC 表面性质的变化应是影响Cd(II)和Ni(II)去除的主要因素. 在较低的初始 pH 情况下(pH 为 2~3), MCBC 表面质子化程度很高, 导致Cd(II)和Ni(II)与 MCBC 间的静电斥力, 使它们很难扩散到 MCBC 表面^[17]; 同时, 大量的 H^+ 与Cd(II)和Ni(II)对 MCBC 表面吸附活性点位的竞争十分激烈^[21]. 当初始 pH 升高至 4~5 范围时, MCBC 表面的质子化程度降低, 致使它与Cd(II)和Ni(II)间的静电斥力减弱, 且 H^+ 浓度的降低也使它与Cd(II)和Ni(II)对吸附活性点位的竞争减小, 从而提高了 MCBC 对Cd(II)和Ni(II)的去除性能及效率. 当初始 pH 大于 4 或 5 时, 液相酸度逐渐接近 MCBC 的 pH_{PZC} [7.42, 图 1(c)], 理论上会使 MCBC 表面的负电荷增多, 增强 MCBC 与Cd(II)和Ni(II)间的引力, 提高Cd(II)和Ni(II)的去除性能^[20]. 实际上, Cd(II)和Ni(II)的去除性能并没有明显的提升, 原因可能是 MCBC 中的Cd(II)和Ni(II)结合位点是恒定的, 这同时说明在研究范围内静电引力不是Cd(II)和Ni(II)去除的主要作用^[22]. 此外, Cd(II)原溶液($100 \text{ mg}\cdot\text{L}^{-1}$)和Ni(II)原溶液($50 \text{ mg}\cdot\text{L}^{-1}$)的 pH 分别为 5.23 和 5.42, 这就意味着将 MCBC 直接投加到原溶液中即可使Cd(II)和Ni(II)被高效地去除. 根据内插法,

此条件下的Cd(II)和Ni(II)的去除量及去除效率分别为 $56.58 \text{ mg}\cdot\text{g}^{-1}$ 及 58.03% 和 $22.85 \text{ mg}\cdot\text{g}^{-1}$ 及 45.69% .

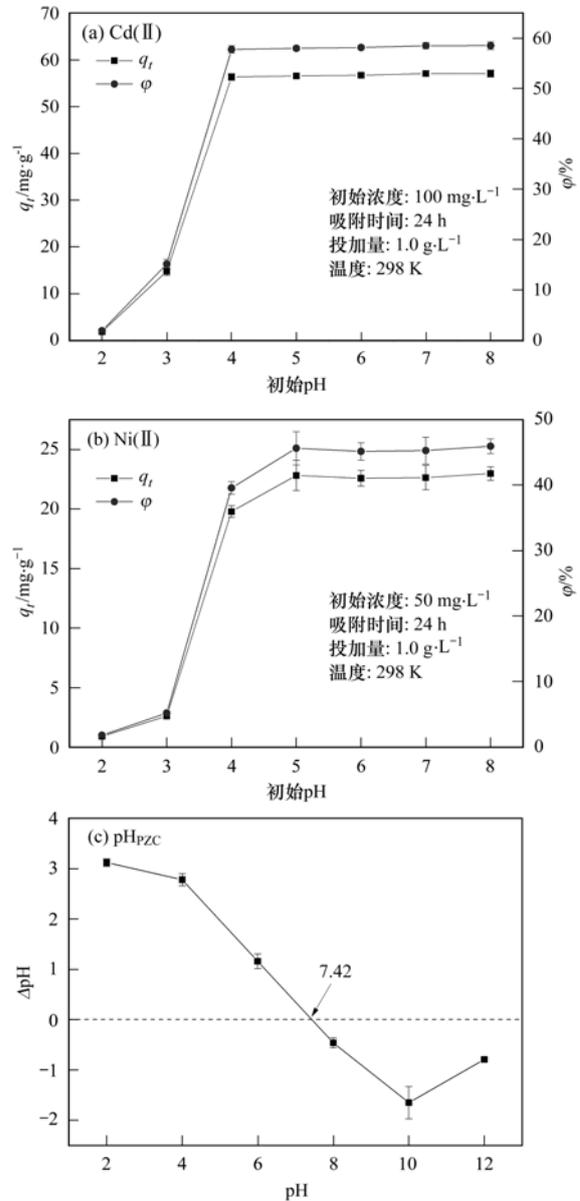


图1 不同 pH 下, Cd(II)和Ni(II)的去除性能及 MCBC 的 pH_{PZC}

Fig. 1 Removal performance of Cd(II) and Ni(II) at different pH and pH_{PZC} of MCBC

2.1.2 投加量的影响

MCBC 投加量对其去除Cd(II)和Ni(II)能力的影响如图 2 所示. 随着投加量从 $0.2 \text{ g}\cdot\text{L}^{-1}$ 增加至 $6 \text{ g}\cdot\text{L}^{-1}$, Cd(II)和Ni(II)的吸附量分别从 $81.90 \text{ mg}\cdot\text{g}^{-1}$ 和 $39.95 \text{ mg}\cdot\text{g}^{-1}$ 下降至 $16.60 \text{ mg}\cdot\text{g}^{-1}$ 和 $8.31 \text{ mg}\cdot\text{g}^{-1}$; 而它们的去除率则分别从 16.38% 和 15.98% 提高至 99.61% 和 99.72% . 这是因为较高的吸附剂投加量能够提供充足的活性点位, 使更多的Cd(II)和Ni(II)被去除; 但这也导致活性点位重叠, 并降低固液界面间Cd(II)和Ni(II)的净通

量,从而降低了 MCBC 对Cd(II)和Ni(II)的吸附量^[18,23]. 由于吸附剂投加量在很大程度上影响污染物去除的成本,所以适宜的 MCBC 投加量建议为 3

$g \cdot L^{-1}$. 在此条件下,MCBC 对Cd(II)和Ni(II)的吸附量及去除率分别为 $33.14 \text{ mg} \cdot g^{-1}$ 及 99.43% 和 $16.53 \text{ mg} \cdot g^{-1}$ 及 99.19% .

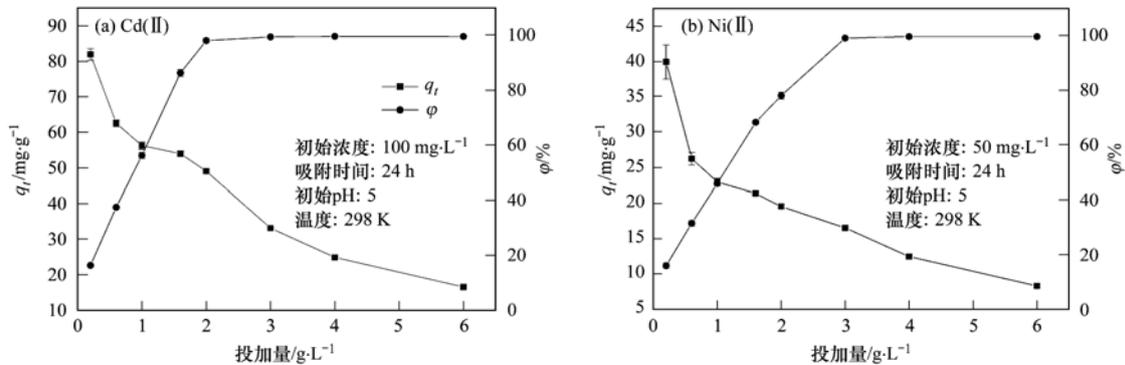


图2 MCBC 投加量对Cd(II)和Ni(II)去除的影响

Fig. 2 Effect of MCBC dosages on Cd(II) and Ni(II) removals

2.2 动力学、等温线和热力学

2.2.1 动力学

MCBC 去除Cd(II)和Ni(II)的动力学拟合结果如图3和表1所示. 由图3(a)、图3(b)和表1可知,Cd(II)和Ni(II)去除的表现动力学较好地遵循了准一级动力学模型和准二级动力学模型;但是,准二级动力学方程的 R^2 值相对更高,分别为

0.9967和0.9857;并且,由准二级动力学方程得到的Cd(II)和Ni(II)的平衡吸附量分别为 $61.06 \text{ mg} \cdot g^{-1}$ 和 $25.88 \text{ mg} \cdot g^{-1}$,与实验结果($q_{e,exp}$)的差距更小. 这些表明,MCBC 对Cd(II)和Ni(II)的去除应是物理吸附和化学吸附的共同作用,且该过程受化学吸附控制,即Cd(II)和Ni(II)与MCBC之间可能通过共用或交换电子形成化学键^[21].

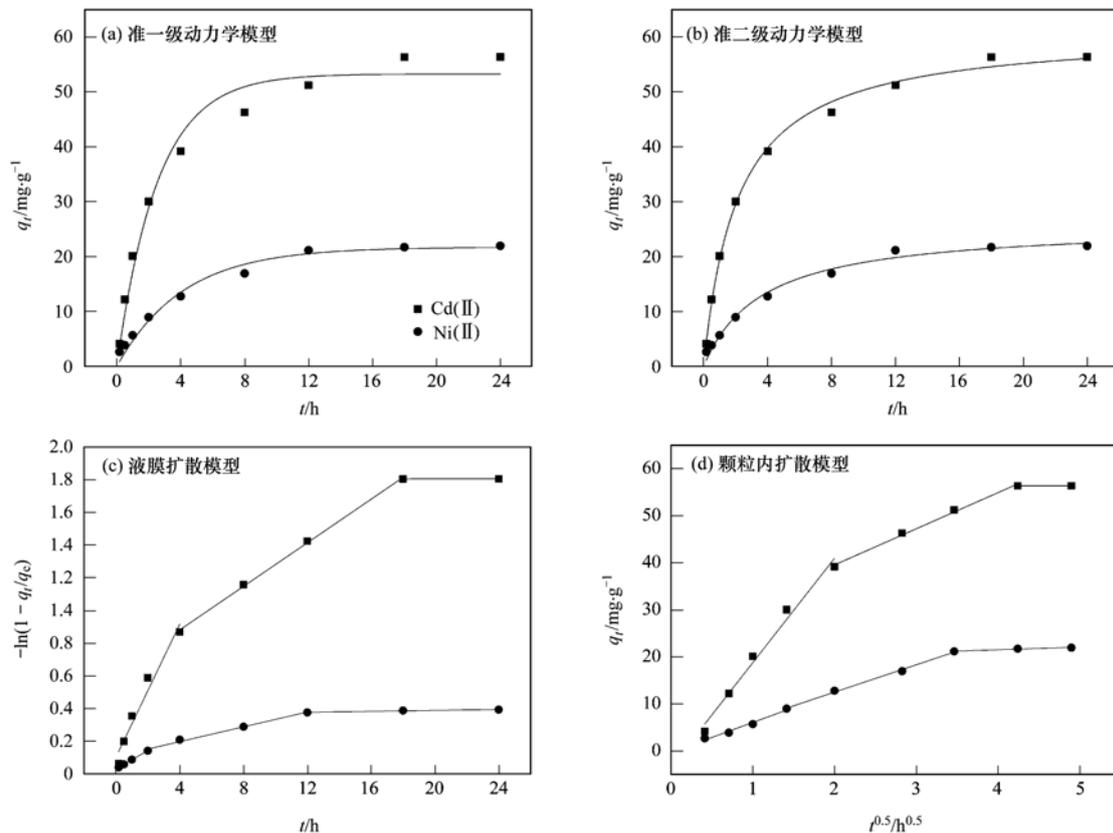


图3 MCBC 去除Cd(II)和Ni(II)的动力学拟合

Fig. 3 Fitting plots of kinetics for Cd(II) and Ni(II) removals by MCBC

从传质过程看[图3(c)和图3(d)],Cd(II)和Ni(II)的去除明显分为3个阶段:快速去除阶段(0

~4 h; 0~2 h)、慢速去除阶段(4~18 h; 2~12 h)和动态平衡阶段或渐近平衡阶段(18~24 h; 12~

表 1 MCBC 去除Cd(II)和Ni(II)的动力学拟合参数

Table 1 Fitting parameters of the kinetics for Cd(II) and Ni(II) removals by MCBC

重金属	$q_{e,exp}$ /mg·g ⁻¹	准一级动力学模型	准二级动力学模型	液膜扩散模型			颗粒内扩散模型		
				第一阶段	第二阶段	第三阶段	第一阶段	第二阶段	第三阶段
Cd(II)	67.45	$q_e = 53.26$	$q_e = 61.06$	$k_{LFD} = 0.2034$	$k_{LFD} = 0.0666$	$k_{LFD} = 1.5E-4$	$k_{IPD} = 22.19$	$k_{IPD} = 7.683$	$k_{IPD} = 0.0152$
		$k_1 = 0.3912$	$k_2 = 0.0077$	$A_L = 0.1031$	$A_L = 0.6148$	$A_L = 1.802$	$A_1 = -3.427$	$A_1 = 24.18$	$A_1 = 56.29$
		$R^2 = 0.9737$	$R^2 = 0.9967$	$R^2 = 0.9468$	$R^2 = 0.9985$	$R^2 = 1.000$	$R^2 = 0.9796$	$R^2 = 0.9940$	$R^2 = 1.000$
Ni(II)	25.05	$q_e = 21.72$	$q_e = 25.88$	$k_{LFD} = 0.0560$	$k_{LFD} = 0.0227$	$k_{LFD} = 0.0014$	$k_{IPD} = 6.363$	$k_{IPD} = 5.812$	$k_{IPD} = 0.5579$
		$k_1 = 0.2427$	$k_2 = 0.0105$	$A_L = 0.0313$	$A_L = 0.1076$	$A_L = 0.3605$	$A_1 = -0.3135$	$A_1 = 0.8675$	$A_1 = 19.27$
		$R^2 = 0.9761$	$R^2 = 0.9857$	$R^2 = 0.9998$	$R^2 = 0.9876$	$R^2 = 0.8989$	$R^2 = 0.9702$	$R^2 = 0.9953$	$R^2 = 0.9361$

24 h). 在第 1 阶段, 由于液相和 MCBC 表面间较高的浓度差, Cd(II) 和 Ni(II) 迅速地穿过液膜扩散到 MCBC 表面, 并与其表面的大量有效吸附点位结合, 发生外表面扩散和表面吸附^[17,24]. 第 2 阶段, 由于固液相间浓度差的降低, 扩散到 MCBC 表面的 Cd(II) 和 Ni(II) 减少; 随着 MCBC 表面的有效吸附点位减少, 吸附在 MCBC 表面的 Cd(II) 和 Ni(II) 逐渐向 MCBC 的孔隙中扩散 (即颗粒内扩散)^[25], 并进行孔隙填充. 第 3 阶段, 随着固液相间浓度差的进一步降低和有效吸附点位逐渐饱和, 整个体系呈现动态平衡或渐近平衡状态. 由表 1 可知, 液膜扩散模型和颗粒内扩散模型的 R^2 值均在可接受范围内, 且 A_L 和 A_1 值均不为零, 表明 Cd(II) 和 Ni(II) 的去除速率由液膜扩散和颗粒内扩散共同决定; 同时, 第 1 阶段的 k_{LFD} 和 k_{IPD} 值远高于第 2 阶段和第 3 阶段, 说明表面吸附是 Cd(II) 和 Ni(II) 去除的控速步

骤^[26].

2.2.2 等温线

Langmuir、Freundlich 和 Temkin 模型对 MCBC 去除 Cd(II) 和 Ni(II) 的等温过程的拟合结果如图 4 和表 2 所示. 从 R^2 值看, Cd(II) 和 Ni(II) 的等温去除更符合 Langmuir 模型, 表明 Cd(II) 和 Ni(II) 主要是以单层形式附着在 MCBC 的表面^[23]. MCBC 对 Cd(II) 和 Ni(II) 的最大吸附量分别为 57.18 mg·g⁻¹ 和 23.34 mg·g⁻¹ (MCBC 投加量为 1 g·L⁻¹; 初始 pH = 5), 与实验结果基本是一致的. 并且, Cd(II) 和 Ni(II) 的分离系数 R_L [$R_L = 1/(1 + K_L \cdot c_0)$] 的范围分别为 0.01 ~ 0.10 和 0.02 ~ 0.30, 说明 MCBC 对 Cd(II) 和 Ni(II) 的去除是有利吸附^[27]. 但是, Cd(II) 去除的 K_L 值大于 Ni(II), 说明 MCBC 对 Cd(II) 的亲合力高于 Ni(II), 更有利于 Cd(II) 的去除^[28].

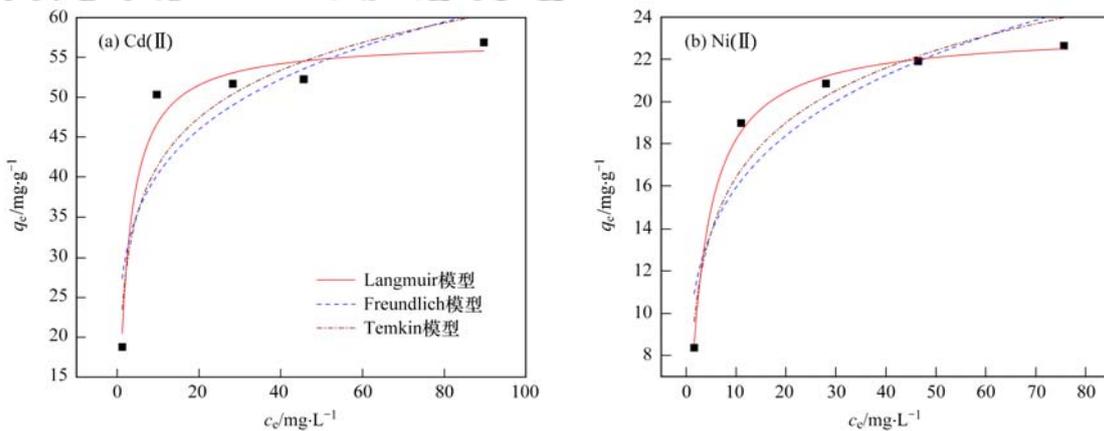


图 4 Langmuir、Freundlich 和 Temkin 模型对 MCBC 去除 Cd(II) 和 Ni(II) 的拟合

Fig. 4 Fitting plots of Langmuir, Freundlich, and Temkin models for Cd(II) and Ni(II) removal by MCBC

表 2 Cd(II) 和 Ni(II) 等温去除的拟合参数

Table 2 Fitting parameters for isothermal removal of Cd(II) and Ni(II)

重金属	$q_{max,exp}$ /mg·g ⁻¹	Langmuir 模型		Freundlich 模型			Temkin 模型			
		q_{max} /mg·g ⁻¹	K_L /L·g ⁻¹	R^2	K_F /(mg·g ⁻¹)·(mg·L ⁻¹) ^{-1/n}	n	R^2	k_T /L·mg ⁻¹	b_T /J·mol ⁻¹	R^2
Cd(II)	55.61	57.18	0.4564	0.9649	26.38	5.394	0.7183	12.67	289.1	0.8263
Ni(II)	24.46	23.34	0.3540	0.9968	9.883	4.823	0.8273	8.006	662.0	0.9165

Temkin 模型拟合 Cd(II) 和 Ni(II) 去除实验数据的 R^2 值分别为 0.8263 和 0.9165, 尚在可接受的

范围内. 这说明 Cd(II) 和 Ni(II) 去除过程的吸附热随着 MCBC 表面覆盖率的增加而降低^[29], 且化学吸

附在Cd(II)和Ni(II)的去除中可能起着重要的作用^[30].这与动力学分析的结论基本是一致的.

2.2.3 热力学

MCBC 去除Cd(II)和Ni(II)的热力学参数如表3所示.负的 ΔG^{\ominus} 值表明在研究范围内MCBC对Cd(II)和Ni(II)的去除是自发的;且 ΔG^{\ominus} 随着温度的升高而降低,说明MCBC对Cd(II)和Ni(II)的去除可能涉及化学反应和温度键合反应^[31].此外,

表3 MCBC去除Cd(II)和Ni(II)的热力学参数

重金属	温度/K	$\Delta G^{\ominus}/\text{kJ}\cdot\text{mol}^{-1}$	$\Delta H^{\ominus}/\text{kJ}\cdot\text{mol}^{-1}$	$\Delta S^{\ominus}/\text{J}\cdot(\text{mol}\cdot\text{K})^{-1}$	R^2
Cd(II)	298	-17.15	19.92	124.4	0.9999
	308	-18.42			
	318	-19.64			
Ni(II)	298	-16.35	12.34	96.03	0.9669
	308	-17.09			
	318	-18.27			

2.3 生物炭表征

2.3.1 SEM

图5展示了Cd(II)和Ni(II)去除前后MCBC的SEM图和表面元素分布情况.从SEM图看出,吸附Cd(II)和Ni(II)后,MCBC表面和孔隙中的颗粒物显著增加,这可能是Cd(II)和Ni(II)成功附着在MCBC上形成的无定形沉淀物^[22].从表面元素分布情况看,Cd和Ni在MCBC表面的颗粒物上有聚集的趋势,证明这些颗粒可能是各种含Cd或Ni的化

Cd(II)的 ΔG^{\ominus} 均低于Ni(II),表明MCBC对Cd(II)的去除需要的能量更少,且自发性更强.Cd(II)和Ni(II)去除的 ΔH^{\ominus} 值分别为 $19.92\text{ kJ}\cdot\text{mol}^{-1}$ 和 $12.34\text{ kJ}\cdot\text{mol}^{-1}$,说明MCBC对Cd(II)和Ni(II)的去除均是吸热的,且物理吸附和化学吸附在它们的去除中均起着重要的作用^[17,32].正的 ΔS^{\ominus} 值表明在Cd(II)和Ni(II)去除过程中,固液界面间的随机性和无序性是增加的^[33].

合物;同时,Cd或Ni的分布与O和Mn的分布具有很好的一致性,说明Cd或Ni可能在MCBC表面形成 $\text{Cd}_n\text{Mn}_m\text{O}_x$ 或 $\text{Ni}_n\text{Mn}_m\text{O}_x$ 类化合物.同时,Cd和Ni在MCBC的表面和孔隙中均有分布,也说明颗粒内扩散在Cd(II)和Ni(II)去除过程中有重要的作用.

2.3.2 XRD

Cd(II)和Ni(II)去除前后MCBC的XRD图谱如图6(a)所示.使用前,MCBC在 2θ 为 $35^{\circ}\sim 40^{\circ}$ 范围内有一个较宽的特征峰,该峰指向锰氧化物 MnO_x (如 MnO 、 MnO_2 、 Mn_2O_3 和 Mn_3O_4 等)^[34~37].吸附Cd(II)和Ni(II)后,MCBC并未有新的晶体结构的特征峰出现,其原因可能是:①Cd和Ni以结晶度低的化合物的形式存在^[35];② MnO_x 对重金属离子有很强的亲和力,能与Cd(II)和Ni(II)形成内球络合物^[37].

2.3.3 FTIR

图6(b)为Cd(II)和Ni(II)去除前后MCBC的FTIR图谱.在吸附Cd(II)和Ni(II)前,MCBC在 3430 、 1630 和 520 cm^{-1} 附近有3个明显的特征峰.它们分别指向O—H伸缩振动^[16]、COO—伸缩振动^[38]和Mn—O伸缩振动^[39].吸附Cd(II)和Ni(II)后,MCBC在 1380 cm^{-1} 附近有新的特征峰形成,其原因可能是Cd(II)和Ni(II)在MCBC上形成内球络合物(Cd—O和Ni—O)^[40].同时,吸附Cd(II)和Ni(II)后,指向Mn—O的伸缩振动峰出现了不同程度的蓝移,可能是Cd(II)和Ni(II)与Mn—O之间发生共沉淀和络合反应^[41].

2.3.4 XPS

去除Cd(II)和Ni(II)前后,MCBC的宽频和精细扫描XPS图谱如图7所示.从MCBC的XPS全谱

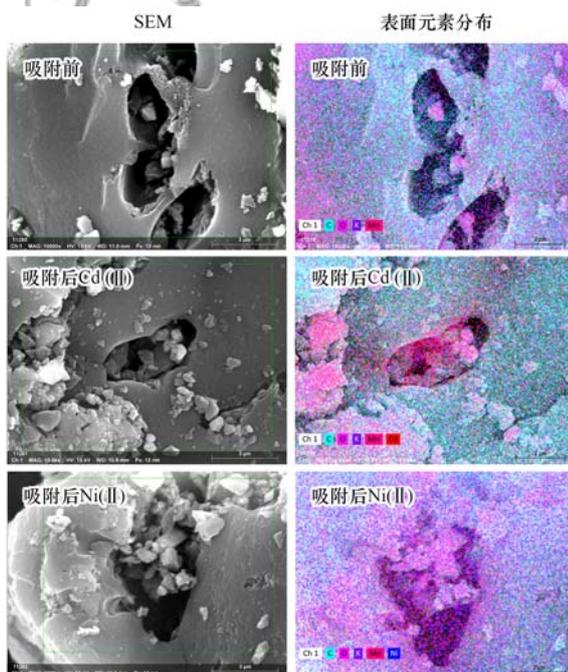


图5 MCBC去除Cd(II)和Ni(II)前后的SEM图和表面元素分布

Fig. 5 SEM images and surface element distribution of MCBC before/after removal of Cd(II) and Ni(II)

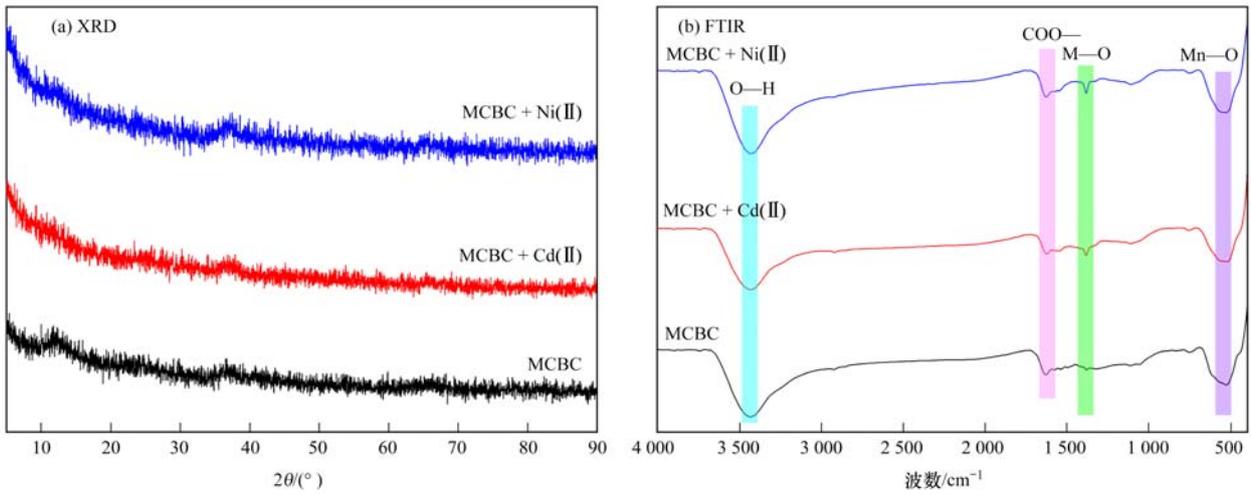


图 6 MCBC 去除Cd(II)和Ni(II)前后的 XRD 图谱和 FTIR 图谱

Fig. 6 XRD patterns and FTIR spectra of MCBC before/after removal of Cd(II) and Ni(II)

图可知[图 7(a)],在吸附Cd(II)和Ni(II)后,MCBC 主要存在的特征峰为 C 1s、O 1s、Mn 2p、Cd 3d 和 Ni 2p,这与 SEM 的结果是一致的.如图 7(b)所示,Mn 2p 在 640.0、(641.4 ± 0.1)、(642.9 ± 0.3) 和 (652.7 ± 0.3) eV 处的特征峰分别与 Mn(II)、Mn(III)、Mn(IV) 和 Mn(II)(MnOOH)

相关^[3,42]; 吸附Cd(II)和Ni(II)后,Mn(II)的峰消失了;同时,Mn(IV)的比例由 27.80% 分别下降至 5.00% 和 0.00%,而 Mn(III)的比例由 28.76% 上升至 45.53% 和 60.16%,表明在Cd(II)和Ni(II)去除过程中还可能存在氧化还原反应;此外,Mn(II)(MnOOH)的比例在吸附Ni(II)后显著减少,说明

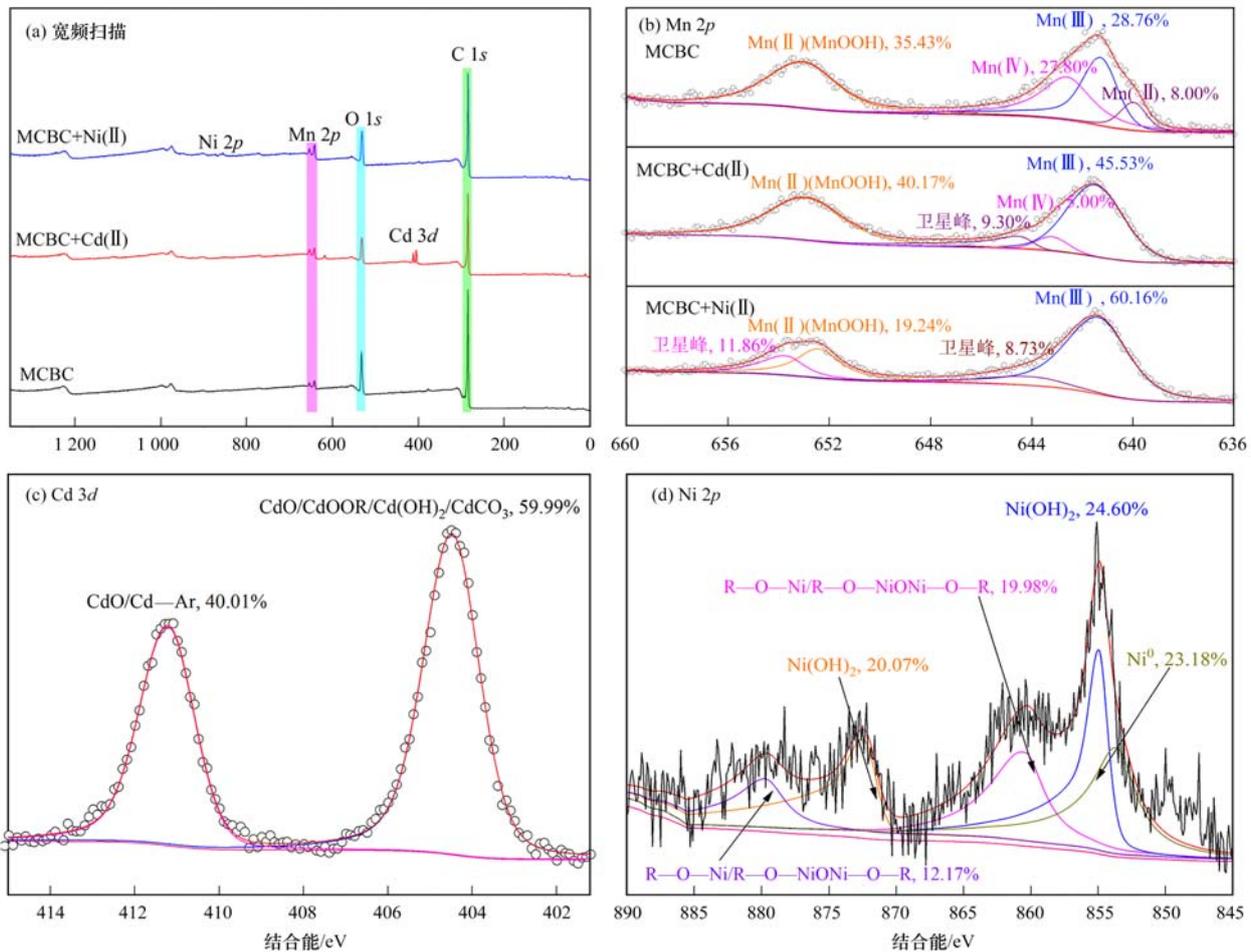


图 7 MCBC 去除Cd(II)和Ni(II)前后的 XPS 分析

Fig. 7 XPS analysis of MCBC before/after Cd(II) and Ni(II) removal

MnOOH 也可能参与了Ni(II)的去除^[42].如图7(c)所示,Cd 3d在404.2 eV和411.7 eV处有两个特征峰,表明Cd可能以CdO、CdOOR、CdCO₃、Cd(OH)₂、Ar—Cd等方式附着在MCBC表面^[17,43].而由图7(d)可知,Ni主要以氢氧化镍(854.9 eV和872.4 eV)、络合氧化镍(860.4 eV和879.7 eV)^[4,44]和Ni⁰(853.6 eV)^[45]的形式固定在MCBC表面.

2.4 Cd(II)和Ni(II)去除的潜在机制

根据实验数据分析(动力学、等温线和热力学分析)、Cd(II)和Ni(II)去除的MCBC表征及相关研究,提出了MCBC去除Cd(II)和Ni(II)的潜在途径和机制(图8).在快速去除阶段,由于固液相间巨

大的含量差(Δc),大量Cd(II)和Ni(II)迅速穿过固液界面间的液膜到达MCBC表面(I:液膜扩散);随后,Cd(II)和Ni(II)又通过表面扩散快速到达吸附点位,完成表面吸附(II:表面扩散和表面吸附);在此阶段,Cd(II)和Ni(II)的去除速率主要由液膜扩散和表面扩散控制.由于固液相间浓度差的降低,扩散至MCBC表面的Cd(II)和Ni(II)减少,Cd(II)和Ni(II)的去除进入慢速去除阶段;同时,由于MCBC表面的活性点位被大量占据,通过物理吸附附着在MCBC表面的Cd(II)和Ni(II)在位势场的作用下向孔隙迁移,实现孔隙填充(III:颗粒内扩散和孔隙填充).当吸附时间超过平衡时间后,Cd(II)和Ni(II)的去除呈动态平衡状态.

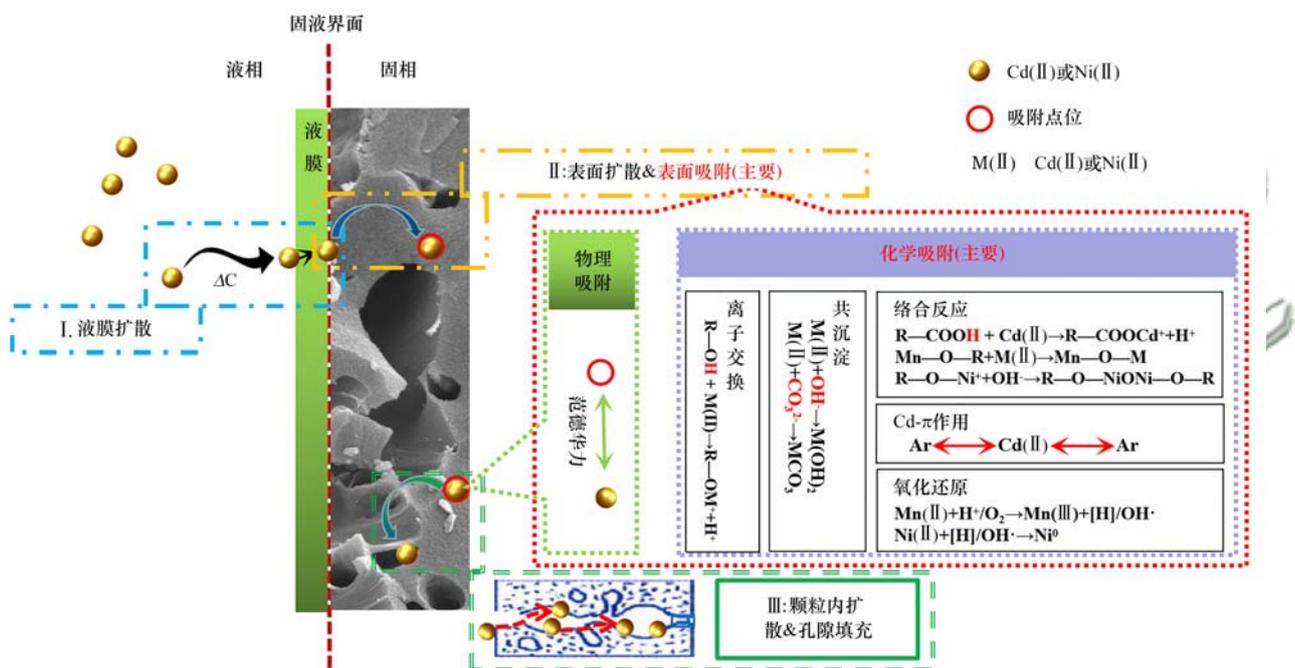


图8 MCBC去除Cd(II)和Ni(II)的潜在机制

Fig. 8 Potential mechanism of Cd(II) and Ni(II) removal by MCBC

MCBC对Cd(II)和Ni(II)的去除主要包括表面吸附和孔隙填充,其中表面吸附对二者去除的贡献更大.而表面吸附既有物理吸附,也有化学吸附;化学吸附是Cd(II)和Ni(II)去除的主要途径.Cd(II)化学吸附去除的方式可能是离子交换、共沉淀、络合反应和阳离子- π 相互作用;而Ni(II)则可能是通过离子交换、共沉淀、络合反应和氧化还原反应被去除的^[3,4,17,45,46].其中,共沉淀和络合作用是Cd(II)和Ni(II)去除的主要方式,而络合产物中无定形的Mn—O—Cd或Mn—O—Ni的占比可能会较高.

3 结论

(1)MCBC对Cd(II)和Ni(II)的去除性能在很

大程度上依赖溶液初始pH和MCBC投加量;当初始pH=5,投加量为3.0 g·L⁻¹时,Cd(II)和Ni(II)的去除率均可达99%以上,相应的吸附量分别为33.14 mg·g⁻¹和16.53 mg·g⁻¹.

(2)Cd(II)和Ni(II)的去除更符合准二级动力学模型,化学吸附是Cd(II)和Ni(II)去除的主要途径;Cd(II)和Ni(II)的去除过程分为快速去除、慢速去除和动态平衡或渐近平衡这3个阶段,其中快速去除阶段为该过程的控速步骤,其速率由液膜扩散和颗粒内扩散共同决定;Cd(II)和Ni(II)的去除方式主要包括表面吸附和孔隙填充,其中表面吸附的贡献更大,MCBC对Cd(II)和Ni(II)的饱和吸附量分别为57.18 mg·g⁻¹和23.29 mg·g⁻¹,约为椰壳生物炭的5.74倍和6.97倍;Cd(II)和

Ni(II) 的去除是自发的、吸热的过程, 具有较为明显的化学吸附热力学特征。

(3) Cd(II) 通过离子交换、共沉淀、络合反应和阳离子- π 相互作用等附着在 MCBC 上; 而 Ni(II) 则是通过离子交换、共沉淀、络合反应和氧化还原反应被 MCBC 去除; 其中, 共沉淀和络合作用是 Cd(II) 和 Ni(II) 去除的主要方式, 且络合产物中无定形的 Mn—O—Cd 或 Mn—O—Ni 的占比可能会较高。

参考文献:

- [1] 王俊杰, 陈晓晨, 李权达, 等. 老化作用对微塑料吸附附的影响及其机制[J]. 环境科学, 2022, **43**(4): 2030-2038.
Wang J J, Chen X C, Li Q D, *et al.* Effects of Aging on the Cd adsorption by microplastics and the relevant mechanisms [J]. *Environmental Science*, 2022, **43**(4): 2030-2038.
- [2] 廖晓峰, 钟静萍, 陈云嫩, 等. 功能化凹凸棒吸附材料的制备及其对重金属废水中 Pb^{2+} 的吸附行为[J]. 环境科学, 2022, **43**(1): 387-397.
Liao X F, Zhong J P, Chen Y N, *et al.* Preparation of functional attapulgite composite and its adsorption behaviors for congo red [J]. *Environmental Science*, 2022, **43**(1): 387-397.
- [3] Tan W T, Zhou H, Tang S F, *et al.* Enhancing Cd(II) adsorption on rice straw biochar by modification of iron and manganese oxides [J]. *Environmental Pollution*, 2022, **300**, doi: 10.1016/j.envpol.2022.118899.
- [4] An Q, Jiang Y Q, Nan H Y, *et al.* Unraveling sorption of nickel from aqueous solution by $KMnO_4$ and KOH-modified peanut shell biochar: implicit mechanism [J]. *Chemosphere*, 2019, **214**: 846-854.
- [5] Amin M T, Alazba A A, Shafiq M. Comparative sorption of nickel from an aqueous solution using biochar derived from banana and orange peel using a batch system: kinetic and isotherm models [J]. *Arabian Journal for Science and Engineering*, 2019, **44**(12): 10105-10116.
- [6] Ong D C, Pingul-Ong S M B, Kan C C, *et al.* Removal of nickel ions from aqueous solutions by manganese dioxide derived from groundwater treatment sludge [J]. *Journal of Cleaner Production*, 2018, **190**: 443-451.
- [7] Yin G C, Song X W, Tao L, *et al.* Novel Fe-Mn binary oxide-biochar as an adsorbent for removing Cd(II) from aqueous solutions [J]. *Chemical Engineering Journal*, 2020, **389**, doi: 10.1016/j.cej.2020.124465.
- [8] Özer Ç, Imamoğlu M. Isolation of Nickel(II) and Lead(II) from aqueous solution by sulfuric acid prepared pumpkin peel biochar [J]. *Analytical Letters*, 2022, doi: 10.1080/00032719.2022.2078981.
- [9] Saravanan A, Senthil Kumar P, Govarthanan M, *et al.* Adsorption characteristics of magnetic nanoparticles coated mixed fungal biomass for toxic Cr(VI) ions in aquatic environment [J]. *Chemosphere*, 2021, **267**, doi: 10.1016/j.chemosphere.2020.129226.
- [10] Bhaumik M, Maity A, Brink H G. Zero valent nickel nanoparticles decorated polyaniline nanotubes for the efficient removal of Pb(II) from aqueous solution: Synthesis, characterization and mechanism investigation [J]. *Chemical Engineering Journal*, 2021, **417**, doi: 10.1016/j.cej.2020.127910.
- [11] Zhou S, Yin J, Ma Q, *et al.* Montmorillonite-reduced graphene oxide composite aerogel (M-rGO): a green adsorbent for the dynamic removal of cadmium and methylene blue from wastewater [J]. *Separation and Purification Technology*, 2022, **296**, doi: 10.1016/j.seppur.2022.121416.
- [12] Egbosiuba T C, Egwunyenga M C, Tijani J O, *et al.* Activated multi-walled carbon nanotubes decorated with zero valent nickel nanoparticles for arsenic, cadmium and lead adsorption from wastewater in a batch and continuous flow modes [J]. *Journal of Hazardous Materials*, 2022, **423**, doi: 10.1016/j.jhazmat.2021.126993.
- [13] Li Y, Gao L M, Lu Z X, *et al.* Enhanced removal of heavy metals from water by hydrous ferric oxide-modified biochar [J]. *ACS Omega*, 2020, **5**(44): 28702-28711.
- [14] Liu C, Zhang H X. Modified-biochar adsorbents (MBAs) for heavy-metal ions adsorption: A critical review [J]. *Journal of Environmental Chemical Engineering*, 2022, **10**(2), doi: 10.1016/j.jece.2022.107393.
- [15] Rajapaksha A U, Chen S S, Tsang D C W, *et al.* Engineered/designer biochar for contaminant removal/immobilization from soil and water: potential and implication of biochar modification [J]. *Chemosphere*, 2016, **148**: 276-291.
- [16] Sun C, Chen T, Huang Q X, *et al.* Enhanced adsorption for Pb(II) and Cd(II) of magnetic rice husk biochar by $KMnO_4$ modification [J]. *Environmental Science and Pollution Research*, 2019, **26**(9): 8902-8913.
- [17] Liu L H, Yue T T, Liu R, *et al.* Efficient absorptive removal of Cd(II) in aqueous solution by biochar derived from sewage sludge and calcium sulfate [J]. *Bioresource Technology*, 2021, **336**, doi: 10.1016/j.biortech.2021.125333.
- [18] Liu L H, Zhao J R, Liu X, *et al.* Reduction and removal of As(V) in aqueous solution by biochar derived from Nano zero-valent-iron (nZVI) and sewage sludge [J]. *Chemosphere*, 2021, **277**, doi: 10.1016/j.chemosphere.2021.130273.
- [19] Alizadeh M, Peighambaroust S J, Foroutan R, *et al.* Surface magnetization of hydrolyzed *Luffa Cylindrica* biowaste with cobalt ferrite nanoparticles for facile Ni^{2+} removal from wastewater [J]. *Environmental Research*, 2022, **212**, doi: 10.1016/j.envres.2022.113242.
- [20] Nikolić V, Tomić N, Bugarčić M, *et al.* Amino-modified hollow alumina spheres; effective adsorbent for Cd^{2+} , Pb^{2+} , As(V), and diclofenac removal [J]. *Environmental Science and Pollution Research*, 2021, **28**(21): 27174-27192.
- [21] 马文艳, 裴鹏刚, 高歌, 等. 微纳米粒径生物炭的结构特征及其对 Cd^{2+} 吸附机制 [J]. 环境科学, 2022, **43**(7): 3682-3691.
Ma W Y, Pei P G, Gao G, *et al.* Structural characteristics of micro-Nano particle size biochar and its adsorption mechanism for Cd^{2+} [J]. *Environmental Science*, 2022, **43**(7): 3682-3691.
- [22] Zhang L X, Tang S Y, He F X, *et al.* Highly efficient and selective capture of heavy metals by poly(acrylic acid) grafted chitosan and biochar composite for wastewater treatment [J]. *Chemical Engineering Journal*, 2019, **378**, doi: 10.1016/j.cej.2019.122215.
- [23] Biswas S, Meikap B C, Sen T K. Adsorptive removal of aqueous phase copper (Cu^{2+}) and nickel (Ni^{2+}) metal ions by synthesized biochar-biopolymeric hybrid adsorbents and process optimization by response surface methodology (RSM) [J]. *Water, Air, & Soil Pollution*, 2019, **230**, doi: 10.1007/s11270-019-4258-y.
- [24] 张立志, 易平, 方丹丹, 等. 超顺磁性纳米 $Fe_3O_4@SiO_2$ 功能化材料对镉的吸附机制 [J]. 环境科学, 2021, **42**(6):

- 2917-2927.
- Zhang L Z, Yi P, Fang D D, *et al.* Adsorption mechanism of cadmium by superparamagnetic nano-Fe₃O₄@SiO₂ functionalized materials [J]. *Environmental Science*, 2021, **42** (6): 2917-2927.
- [25] Zhang S Y, Arkin K, Zheng Y X, *et al.* Preparation of a composite material based on self-assembly of biomass carbon dots and sodium alginate hydrogel and its green, efficient and visual adsorption performance for Pb²⁺ [J]. *Journal of Environmental Chemical Engineering*, 2022, **10** (1), doi: 10.1016/j.jece.2021.106921.
- [26] Liu B X, Chen T, Wang B, *et al.* Enhanced removal of Cd²⁺ from water by AHP-pretreated biochar: adsorption performance and mechanism [J]. *Journal of Hazardous Materials*, 2022, **438**, doi: 10.1016/j.jhazmat.2022.129467.
- [27] Zandi-Mehri E, Taghavi L, Moeinpour F, *et al.* Designing of hydroxyl terminated triazine-based dendritic polymer/halloysite nanotube as an efficient nano-adsorbent for the rapid removal of Pb(II) from aqueous media [J]. *Journal of Molecular Liquids*, 2022, **360**, doi: 10.1016/j.molliq.2022.119407.
- [28] 马凯悦, 张浩, 宋宁宁, 等. 氧化老化玉米秸秆生物炭吸附镉机理研究 [J]. *农业环境科学学报*, 2022, **41** (6): 1230-1240.
- Ma K Y, Zhang H, Song N N, *et al.* Mechanism of cadmium adsorption by oxidative aging corn straw biochar [J]. *Journal of Agro-Environment Science*, 2022, **41** (6): 1230-1240.
- [29] Jiang L, Chen Y T, Wang Y F, *et al.* Contributions of various Cd(II) adsorption mechanisms by *Phragmites australis*-activated carbon modified with mannitol [J]. *ACS Omega*, 2022, **7** (12): 10502-10515.
- [30] Gao Y S, Qi G S, Yan W C, *et al.* Preparation of L-cysteine modified MnFe₂O₄ nanoparticles based on high-gravity technology and application for the removal of lead [J]. *Journal of Environmental Chemical Engineering*, 2022, **10** (2), doi: 10.1016/j.jece.2022.107193.
- [31] 胡美艳, 张翔凌, 姬筠森, 等. 两种碳酸系 Fe-LDHs 负载改性沸石对 Cd(II) 吸附特性对比研究 [J]. *环境科学研究*, 2021, **34** (11): 2655-2664.
- Hu M Y, Zhang X L, Ji Y S, *et al.* Comparison of adsorption mechanisms of modified zeolite coated with two different Fe-CO₃-layered double hydroxides for Cd(II) removal [J]. *Research of Environmental Science*, 2021, **34** (11): 2655-2664.
- [32] Narasimharao K, Lingamdinne L P, Al-Thabaiti S, *et al.* Synthesis and characterization of hexagonal Mg-Fe layered double hydroxide/grapheme oxide nanocomposite for efficient adsorptive removal of cadmium ion from aqueous solutions: Isotherm, kinetic, thermodynamic and mechanism [J]. *Journal of Water Process Engineering*, 2022, **47**, doi: 10.1016/j.jwpe.2022.102746.
- [33] Iamsaard K, Weng C H, Yen L T, *et al.* Adsorption of metal on pineapple leaf biochar: key affecting factors, mechanism identification, and regeneration evaluation [J]. *Bioresource Technology*, 2022, **344**, doi: 10.1016/j.biortech.2021.126131.
- [34] Gao B X, Zhu S M, Gu J L, *et al.* Superoxide radical mediated Mn(III) formation is the key process in the activation of peroxymonosulfate (PMS) by Mn-incorporated bacterial-derived biochar [J]. *Journal of Hazardous Materials*, 2022, **431**, doi: 10.1016/j.jhazmat.2022.128549.
- [35] Deng H, Zhang J Y, Huang R, *et al.* Adsorption of malachite green and Pb²⁺ by KMnO₄-modified biochar: insights and mechanisms [J]. *Sustainability*, 2022, **14** (4), doi: 10.3390/su14042040.
- [36] Huang D L, Zhang Q, Zhang C, *et al.* Mn doped magnetic biochar as persulfate activator for the degradation of tetracycline [J]. *Chemical Engineering Journal*, 2020, **391**, doi: 10.1016/j.cej.2019.123532.
- [37] Qiu Y, Zhang Q, Li M, *et al.* Adsorption of Cd(II) From aqueous solutions by modified biochars: comparison of modification methods [J]. *Water, Air, & Soil Pollution*, 2019, **230** (4), doi: 10.1007/s11270-019-4135-8.
- [38] Liang R H, Li Y, Huang L, *et al.* Pb²⁺ adsorption by ethylenediamine-modified pectins and their adsorption mechanisms [J]. *Carbohydrate Polymers*, 2020, **234**, doi: 10.1016/j.carbpol.2020.115911.
- [39] Li N, Yin M L, Tsang D C W, *et al.* Mechanisms of U(VI) removal by biochar derived from *Ficus microcarpa* aerial root: a comparison between raw and modified biochar [J]. *Science of the Total Environment*, 2019, **697**, doi: 10.1016/j.scitotenv.2019.134115.
- [40] He C X, Xie F C. Adsorption behavior of manganese dioxide towards heavy metal ions: surface zeta potential effect [J]. *Water, Air, & Soil Pollution*, 2018, **229** (3), doi: 10.1007/s11270-018-3712-6.
- [41] Yang T T, Xu Y M, Huang Q Q, *et al.* Removal mechanisms of Cd from water and soil using Fe-Mn oxides modified biochar [J]. *Environmental Research*, 2022, **212**, doi: 10.1016/j.envres.2022.113406.
- [42] Yuan L, Wen J, Xue Z Z, *et al.* Microscopic investigation into remediation of cadmium and arsenite Co-contamination in aqueous solution by Fe-Mn-incorporated titanasilicate [J]. *Separation and Purification Technology*, 2021, **279**, doi: 10.1016/j.seppur.2021.119809.
- [43] Guo J H, Yan C Z, Luo Z X, *et al.* Synthesis of a novel ternary HA/Fe-Mn oxides-loaded biochar composite and its application in cadmium(II) and arsenic(V) adsorption [J]. *Journal of Environmental Sciences*, 2019, **85**: 168-176.
- [44] Li L, Chang K K, Fang P, *et al.* Highly efficient scavenging of Ni(II) by porous hexagonal boron nitride: kinetics, thermodynamics and mechanism aspects [J]. *Applied Surface Science*, 2020, **521**, doi: 10.1016/j.apsusc.2020.146373.
- [45] Wu J, Yi Y Q, Li Y Q, *et al.* Excellently reactive Ni/Fe bimetallic catalyst supported by biochar for the remediation of decabromodiphenyl contaminated soil: reactivity, mechanism, pathways and reducing secondary risks [J]. *Journal of Hazardous Materials*, 2016, **320**: 341-349.
- [46] Teng D Y, Zhang B B, Xu G M, *et al.* Efficient removal of Cd(II) from aqueous solution by pinecone biochar: sorption performance and governing mechanisms [J]. *Environmental Pollution*, 2020, **265**, doi: 10.1016/j.envpol.2020.115001.

CONTENTS

Research Status and Trend Analysis of Environmental and Health Risk and Control of Persistent, Mobile, and Toxic Chemicals	ZHANG Shao-xuan, CHEN An-na, CHEN Cheng-kang, <i>et al.</i> (3017)
Assessment of the Multidimensional Performances of Food Waste Utilization Technologies in China	YANG Guang, SHI Bo-fen, ZHOU Chuan-bin (3024)
Spatial Network of Urban Heat Environment in Beijing-Tianjin-Hebei Urban Agglomeration Based on MSPA and Circuit Theory	QIAO Zhi, CHEN Jia-yue, WANG Nan, <i>et al.</i> (3034)
Relationship Between Urban Spatial Pattern and Thermal Environment Response in Summer: A Case Study of Hefei City	CHEN Yuan-yuan, YAO Xia-mei, OU Chun, <i>et al.</i> (3043)
Assessment of Emission Reduction Effect of Major Air Pollution Control Measures on PM _{2.5} Concentrations During 13th Five-Year Period in Tianjin	XIAO Zhi-mei, XU Hong, CAI Zi-ying, <i>et al.</i> (3054)
Effect of Clean Heating on Carbonaceous Aerosols in PM _{2.5} During the Heating Period in Baoding	LUO Yu-qian, ZHANG Kai, ZHAO Yu-xi, <i>et al.</i> (3063)
Transport Influence and Potential Sources of PM _{2.5} Pollution for Nanjing	XIE Fang-jian, ZHENG Xin-mei, DOU Tao-tao, <i>et al.</i> (3071)
Impact of Atmospheric Circulation Patterns on Ozone Changes in the Pearl River Delta from 2015 to 2020	WANG Yao, LIU Run, XIN Fan (3080)
Effects of Tropical Cyclones on Ozone Pollution in Hainan Island	FU Chuan-bo, DAN Li, TONG Jin-he, <i>et al.</i> (3089)
Analysis of Causes and Sources of Summer Ozone Pollution in Rizhao Based on CMAQ and HYSPLIT Models	LIN Xin, TONG Ji-long, WANG Yi-fan, <i>et al.</i> (3098)
Health Benefit Evaluation for PM _{2.5} as Well as O ₃ _{8h} Pollution Control in Chengdu, China from 2016 to 2020	ZHANG Ying, TIAN Qi-qi, WEI Xiao-yu, <i>et al.</i> (3108)
Impacts of COVID-19 Lockdown on Air Quality in Shenzhen in Spring 2022	LIU Chan-fang, ZHANG Ao-xing, FANG Qing, <i>et al.</i> (3117)
Emission Inventory of Airborne Pollutants from Biomass Combustion in Guizhou Province	WANG Yan-ni, YANG Jing-ting, HUANG Xian-feng, <i>et al.</i> (3130)
Main Chemical Components in Atmospheric Precipitation and Their Sources in Xi'an	ZHOU Dong, HUANG Zhi-pu, LI Si-min, <i>et al.</i> (3142)
Distribution, Respiratory Exposure, and Traceability of Atmospheric Microplastics in Yichang City	LIU Li-ming, WANG Chao, GONG Wen-wen, <i>et al.</i> (3152)
Hydrochemical Evolution in the Yarlung Zangbo River Basin	JIANG Ping, ZHANG Quan-fa, LI Si-yue (3165)
Temporal and Spatial Distribution Characteristics and Source Analysis of Nitrate in Surface Water of Wuding River Basin	XU Qi-feng, XIA Yun, LI Shu-jian, <i>et al.</i> (3174)
Seasonal Variation Characteristics and Pollution Assessment of Heavy Metals in Water and Sediment of Taipu River	LUO Peng-cheng, TU Yao-jen, SUN Ting-ting, <i>et al.</i> (3184)
Pollution Characteristics and Risk Assessment of Antibiotics in Beiyun River Basin in Beijing	JIANG Bao, SUI Shan-shan, SUN Cheng-yi, <i>et al.</i> (3198)
Tracking Riverine Nitrate Sources and Transformations in the Yiluo River Basin by Nitrogen and Oxygen Isotopes	GUO Wen-jing, ZHANG Dong, JIANG Hao, <i>et al.</i> (3206)
Distribution Characteristics and Risk Assessment of PPCPs in Surface Water and Sediments of Lakes in the Lower Reaches of the Huaihe River	WU Yu-sheng, HUANG Tian-yin, ZHANG Jia-gen, <i>et al.</i> (3217)
Characteristics and Driving Mechanisms of Shallow Groundwater Chemistry in Xining City	LIU Chun-yan, YU Kai-ning, ZHANG Ying, <i>et al.</i> (3228)
Groundwater Pollution Risk Assessment in Plain Area of the Yarkant River Basin	YAN Zhi-yun, ZENG Yan-yan, ZHOU Jin-long, <i>et al.</i> (3237)
Composition Structure and Influence Factors of Bacterial Communities in the Miyun Reservoir	CHEN Ying, WANG Jia-wen, LIANG En-hang, <i>et al.</i> (3247)
Photo-Degradation Mechanism and Pathway for Tetracycline in Simulated Seawater Under Irradiation of Visible Light	XU Heng-tao, FU Xiao-hang, FENG Wei-hua, <i>et al.</i> (3260)
Adsorption Characteristics and Mechanism of Ammonia Nitrogen in Water by Nano Zero-valent Iron-modified Biochar	CHEN Wen-jing, SHI Jun-ling, LI Xue-ting, <i>et al.</i> (3270)
Removal Performance and Mechanism of Potassium Permanganate Modified Coconut Shell Biochar for Cd(II) and Ni(II) in Aquatic Environment	ZHANG Feng-zhi, WANG Dun-qiu, CAO Xing-feng, <i>et al.</i> (3278)
Phosphorus Adsorption in Water and Immobilization in Sediments by Lanthanum-modified Water Treatment Sludge Hydrochar	HE Li-wenze, CHEN Yu, SUN Fei, <i>et al.</i> (3288)
Factors Affecting Nitrate Concentrations and Nitrogen and Oxygen Isotope Values of Effluents from Waste Water Treatment Plant	ZHANG Dong, GE Wen-biao, ZHAO Ai-ping, <i>et al.</i> (3301)
Effects of Wastewater Treatment Processes on the Removal Efficiency of Microplastics Based on Meta-analysis	FU Li-song, HOU Lei, WANG Yan-xia, <i>et al.</i> (3309)
Assessment of Critical Loads of Nitrogen Deposition in Natural Ecosystems of China	HUANG Jing-wen, LIU Lei, YAN Xiao-yuan, <i>et al.</i> (3321)
Impacts of Climate Change and Human Activities on NDVI Change in Eastern Coastal Areas of China	JIN Yan-song, JIN Kai, WANG Fei, <i>et al.</i> (3329)
Ecosystem Carbon Storage in Hangzhou Bay Area Based on InVEST and PLUS Models	DING Yue, WANG Liu-zhu, GUI Feng, <i>et al.</i> (3343)
Soil Stoichiometry Characterization in the Oasis-desert Transition Zone of Linze, Zhangye	SUN Xue, LONG Yong-li, LIU Le, <i>et al.</i> (3353)
Vertical Differences in Grassland Bacterial Community Structure During Non-Growing Season in Eastern Ulansuhai Basin	LI Wen-bao, ZHANG Bo-yao, SHI Yu-jiao, <i>et al.</i> (3364)
Distribution Pattern of Bacterial Community in Soil Profile of <i>Larix principis-rupprechtii</i> Forest in Luya Mountain	MAO Xiao-ya, LIU Jin-xian, JIA Tong, <i>et al.</i> (3376)
Effects of Vegetation Types on Carbon Cycle Functional Genes in Reclaimed Soil from Open Pit Mines in the Loess Plateau	ZHAO Jiao, MA Jing, ZHU Yan-feng, <i>et al.</i> (3386)
Effects of Biochar Application on Soil Bacterial Community Diversity and Winter Wheat Growth in Wheat Fields	YAO Li-ru, LI Wei, ZHU Yuan-zheng, <i>et al.</i> (3396)
Effects of Different Planting Years of <i>Dendrocalamus brandisii</i> on Soil Fungal Community	ZHU Shu-hong, HUI Chao-mao, ZHAO Xiu-ting, <i>et al.</i> (3408)
Effects of Biochar Amendment on N ₂ O Emission and Its Functional Genes in Pepper Growing Soil in Tropical Areas	CHEN Qi-qi, WANG Zi-jun, CHEN Yun-zhong, <i>et al.</i> (3418)
Effects of Mulching and Application of Organic and Chemical Fertilizer on Greenhouse Gas Emission and Water and Nitrogen Use in Summer Maize Farmland	JIANG Hong-li, LEI Qi, ZHANG Biao, <i>et al.</i> (3426)
Effects of Different Types of Plastic Film Mulching on Soil Quality, Root Growth, and Yield	MU Xiao-guo, GAO Hu, LI Mei-hua, <i>et al.</i> (3439)
Pollution Assessment and Source Analysis of Heavy Metals in Atmospheric Deposition in a Lead-zinc Smelting City Based on PMF Model	CHEN Ming, WANG Lin-ling, CAO Liu, <i>et al.</i> (3450)
Characterization and Health Risk of Heavy Metals in PM _{2.5} from Road Fugitive Dust in Five Cities of Yunnan Province	HAN Xin-yu, GUO Jin-yuan, SHI Jian-wu, <i>et al.</i> (3463)
Pollution Characteristics and Risk Assessment of Heavy Metals in Surface Dusts and Surrounding Green Land Soils from Yellow River Custom Tourist Line in Lanzhou	LI Jun, LI Kai-ming, WANG Xiao-huai, <i>et al.</i> (3475)
Source Apportionment and Pollution Assessment of Soil Heavy Metal Pollution Using PMF and RF Model: A Case Study of a Typical Industrial Park in Northwest China	GAO Yue, LÜ Tong, ZHANG Yun-kai, <i>et al.</i> (3488)
Source Analysis of Soil Heavy Metals in Agricultural Land Around the Mining Area Based on APCS-MLR Receptor Model and Geostatistical Method	ZHANG Chuan-hua, WANG Zhong-shu, LIU Li, <i>et al.</i> (3500)
Source Analysis of Heavy Metals in Typical Farmland Soils Based on PCA-APCS-MLR and Geostatistics	WANG Mei-hua (3509)
Characteristics and Risk Evaluation of Heavy Metal Contamination in Paddy Soils in the Three Gorges Reservoir Area	LIU Ya-jun, LI Cai-xia, MEI Nan, <i>et al.</i> (3520)
Health Risk Assessment and Environmental Benchmark of Heavy Metals in Cultivated Land in Wanjiang Economic Zone	LIU Hai, WEI Wei, SONG Yang, <i>et al.</i> (3531)
Evaluation and Source Analysis of Soil Heavy Metal Pollution in a Planting Area in Wanquan District, Zhangjiakou City	AN Yong-long, YIN Xiu-lan, LI Wen-juan, <i>et al.</i> (3544)
Heavy Metal Concentration, Source, and Pollution Assessment in Topsoil of Chuzhou City	TANG Jin-lai, ZHAO Kuan, HU Rui-xin, <i>et al.</i> (3562)
Analysis on the Distribution Characteristics and Influence Mechanism of Migration and Transformation of Heavy Metals in Mining Wasteland	WEI Hong-bin, LUO Ming, XIANG Lei, <i>et al.</i> (3573)
Ecological Risk Assessment and Source Apportionment of Heavy Metals in Mineral Resource Base Based on Soil Parent Materials	WEI Xiao-feng, SUN Zi-jian, CHEN Zi-ran, <i>et al.</i> (3585)
Enrichment Characteristics of Heavy Metals and Health Risk in Different Vegetables	QI Hao, ZHUANG Jian, ZHUANG Zhong, <i>et al.</i> (3600)
Health Risk Assessment of Heavy Metals in Soil and Wheat Grain in the Typical Sewage Irrigated Area of Shandong Province	WANG Fei, FEI Min, HAN Dong-nui, <i>et al.</i> (3609)
Prediction of Cadmium Uptake Factor in Wheat Based on Machine Learning	NIU Shuo, LI Yan-ling, YANG Yang, <i>et al.</i> (3619)